Author's Accepted Manuscript

www.elsevier.com

A nearly uniform distributional pattern of heterotrophic bacteria in the Mariana Trench interior

Jiwei Tian, Lu Fan, Haodong Liu, Jiwen Liu, Yi Li, Qilong Qin, Zheng Gong, Hongtao Chen, Zhongbin Sun, Li Zou, Xuchen Wang, Hongzhou Xu, Douglas Bartlett, Min Wang, Yu-Zhong Zhang, Xiao-Hua Zhang, Chuanlun L. Zhang

PII: S0967-0637(18)30240-1
DOI: https://doi.org/10.1016/j.dsr.2018.10.002
Reference: DSRI2967

To appear in: *Deep-Sea Research Part I*

Received date: 7 August 2018
Revised date: 30 September 2018
Accepted date: 4 October 2018

Cite this article as: Jiwei Tian, Lu Fan, Haodong Liu, Jiwen Liu, Yi Li, Qilong Qin, Zheng Gong, Hongtao Chen, Zhongbin Sun, Li Zou, Xuchen Wang, Hongzhou Xu, Douglas Bartlett, Min Wang, Yu-Zhong Zhang, Xiao-Hua Zhang and Chuanlun L. Zhang, A nearly uniform distributional pattern of heterotrophic bacteria in the Mariana Trench interior, *Deep-Sea Research Part I,* https://doi.org/10.1016/j.dsr.2018.10.002

This is a PDF file of an unedited manuscript that has been accepted for publication. As a service to our customers we are providing this early version of the manuscript. The manuscript will undergo copyediting, typesetting, and review of the resulting galley proof before it is published in its final citable form. Please note that during the production process errors may be discovered which could affect the content, and all legal disclaimers that apply to the journal pertain.

ACCEPTED MANUSCRIPT

A nearly uniform distributional pattern of heterotrophic bacteria in the Mariana Trench interior

Jiwei Tian[a1*], Lu Fan[b,c1*], Haodong Liu[d], Jiwen Liu[e], Yi Li[f], Qilong Qin[f], Zheng Gong[e], Hongtao Chen[g], Zhongbin Sun[a], Li Zou[h], Xuchen Wang[g], Hongzhou Xu[i], Douglas Bartlett[j], Min Wang[e], Yu-Zhong Zhang[f], Xiao-Hua Zhang[e], Chuanlun L. Zhang[b,k]

[a]Key Laboratory of Physical Oceanography, Ocean University of China, Qingdao 266100, China

[b]Shenzhen Key Laboratory of Marine Archaea Geo-Omics, Department of Ocean Science and Engineering, Southern University of Science and Technology, Shenzhen 518055, China

[c]SUSTech Academy for Advanced Interdisciplinary Studies, Southern University of Science and Technology, Shenzhen 518055, China

[d]State Key Laboratory of Marine Geology, Tongji University, Shanghai 200092 China

[e]College of Marine Life Sciences, Ocean University of China, Qingdao 266003, China

[f]State Key Laboratory of Microbial Technology, Marine Biotechnology Research Center, Shandong University, Jinan 250100, China

[g]College of Chemistry and Chemical Engineering, Ocean University of China, Qingdao, 266100, China

[g]Key Laboratory of Marine Environmental Science and Ecology, Ocean University of China, Qingdao, 266100, China

[h]Institute of Deep-Sea Science and Engineering, Chinese Academy of Sciences, Sanya 572000, China

[h]Marine Biology Research Division, Scripps Institution of Oceanography, University of California San Diego, La Jolla, California, United States of America

[i]Laboratory for Marine Geology, Qingdao Pilot National Laboratory for Marine Science and Technology, Qingdao, 266061, China

[1] These authors contributed equally to this study

Accepted manuscript

ACCEPTED MANUSCRIPT

tianjw@ouc.edu.cn
fanl@sustc.edu.cn

*Corresponding author. Key Laboratory of Physical Oceanography, Ocean University of China, Qingdao 266100, China
*Corresponding author. Department of Ocean Science and Engineering, Southern University of Science and Technology, Shenzhen 518055, China

Abstract

The uniqueness of hadal trench environment and its potential role in global carbon sequestration allows for a detailed study of microbially driven carbon cycle of the trench system. Limited studies on microbiology by far have suggested that the hadal-sphere generally hosts a heterotrophic microbial community that is mostly fed by surface-sinking organic matter or re-suspended and laterally transported organic matter from sediments. However, temporal dynamics in trench microbial community in connection to surface and sediment organic carbon exports is still beyond our knowledge. In this study, we conducted vertical sampling and analysis of the microbial community from the epipelagic zone down to the hadal zone at the Mariana Trench. 16S rRNA gene composition showed high variations at the first 1000 meters below surface (mbs); however, a nearly uniform microbial community composition (Jaccard dissimilarity less than 73%) was observed below 1000 mbs and down into the bottom of the trench. The deep-sea bacteria were generally chemoheterotrophs characterized by *Erythrobacter*, *Rhodovulum*, *Alteromonas*, some *Marinobacter*, etc., which were also present at the ocean surface. Several deep-sea-enriched but surface-depleted bacteria include *Glaciecola*, *Oceanicola* and *Oleibacter* were potential degraders of large organic polymers. In spite of consistent community composition, enhanced chromophoric dissolved organic matter proportions in the hadal zone of the trench might imply intensified microbial activity compared to the water column above. These observations suggest an unusual transitory state of the Mariana Trench water columns and extend our understanding of the dynamics of the hadal microbial community.

Accepted manuscript

ACCEPTED MANUSCRIPT

Keywords: Mariana Trench; hadal environment; archaea and bacteria; biogeochemistry; organic matter

1 Introduction

The hadal zone commonly refers to the deepest areas of the ocean between 6,000 and approximately 11,000 m. Hadal trenches are part of the least investigated biosphere on Earth due to the great challenge of sampling (Liu *et al.*, 2017). So far, its geological, physical, chemical, and biological processes remain largely unknown.

Hadal microbial communities are of great scientific interest due to their significant role in global carbon cycle. However, only recently, we are able to have a holistic view of the diversity and functional potential of hadal microbial communities. Eloe *et al*. (2011a,b) and Leon-Zayas *et al*. (2015) reported on the planktonic microbial community in the Puerto Rico Trench, followed by studies of the Mariana (Nunoura *et al.*, 2015; Tarn *et al.*, 2016) and the Japan Trench (Nunoura *et al.*, 2016). These studies all indicated distinct hadal communities different from the upper water column, which may be attributed to the unique benthic processes influenced by trench geomorphology, hydrography and slope sediment dynamics intimately fueling the microorganisms in the trench system (Nunoura *et al.*, 2015). Similarly, enhanced microbial turnover rates in shallow sediments of the Mariana Trench were attributed to sedimentary process-driven availability of organic matter in the trench environment (Glud *et al.*, 2013). Mathematic models suggested that either topography, hydrography, or a combination of these factors determines the hadal zone as a relatively nutrient-enriched environment compared to the above abyssopelagic ocean (Ichino *et al.*, 2015). Specifically, near bottom hydrological activities (Turnewitsch *et al.*, 2014), frequent earthquakes and volcanic eruptions (Oguri *et al.*, 2013), and dynamic nutrient input from the ocean's surface (Reinthaler *et al.*, 2006) may all have significant impact on the nature of trench microbial communities.

Particle-associated and free-living microbial communities are phylogenetically (Eloe *et al.*, 2011b) and functionally (Moeseneder *et al.*, 2001; Lauro and Bartlett, 2008) different in the dark ocean. In the Puerto Rico Trench, the particle-associated bacterial fraction (> 3 μm) hosts a greater diversity compared with the free-living fraction (0.22 to 3 μm) and is distinct in community composition (Eloe *et al.*, 2011b). However, the archaeal fractions are not significantly different. In the Mariana Trench, higher

Accepted manuscript

ACCEPTED MANUSCRIPT

diversity was found in the 0.22 to 3 μm fraction compared to that of the > 3 μm and 0.1 to 0.22 μm fractions (Tarn *et al.*, 2016).

While inter-trench heterogeneity, especially between trenches under oligotrophic and eutrophic oceans, has be noticed in several recent studies (Fujii *et al.*, 2013; Yoshida *et al.*, 2013; Turnewitsch *et al.*, 2014; Gallo *et al.*, 2015; Lacey *et al.*, 2016; Wenzhöfer *et al.*, 2016; Nunoura *et al.*, 2016), temporal dynamics of the trench biosphere is still poorly examined. Specifically, short-term phytodetrital pulses contribute substantially to the export of both organic carbon and nutritious compounds into the ocean interior (Fabiano *et al.*, 2001; Gibson *et al.*, 2003; Christina and Passow, 2007) and introduce large-scale changes in bathyl (Ruhl and Smith, 2004) and abyssal (Ruhl *et al.*, 2008) communities. Their impact may extend to the even deeper hadal zones when the flux is strong. Therefore, so far, the very limited reports of the planktonic microbial populations at the Mariana Trench only provides us a partial picture of the real trench biodiversity. We hypothesize that our further sampling efforts may offer a different temporal nature of the Mariana Trench hadal microbial community.

As part of the 'Marathon (Mariana Trench Observation) Program', we conducted vertical sampling of microbial communities of the oligotrophic Mariana Trench. Bacterial and archaeal cells were collected in two size fractions and community composition was analyzed based on their 16S ribosomal RNA (rRNA) genes. We compared the hadal microbial communities to both the overlain counterparts and those reported by Nunoura *et al*. (2015) to reveal intra-trench and temporal heterogeneity of the microbial communities at the Mariana Trench.

2 Material and methods

2.1 Temperature and seawater chemistry measurements

Sampling was conducted at the Challenger Deep of the Mariana Trench (11°22.569'N, 142°18.105'E) in December 2015 (**Fig. 1**). The sampling station was about 46 km west of that in the study conducted by Nunoura *et al.* (2015). Surface water (~ 2 m deep) was collected by using a submerged pump. The deeper water samples were collected by using a custom-designed eight-12 liter Niskin bottle system equipped with a conductivity-temperature-depth (CTD) device down to 8727 m below surface (mbs). Depth, temperature and salinity were continuously recorded by the CTD.

Accepted manuscript

ACCEPTED MANUSCRIPT

In situ measurement of dissolved oxygen (DO) was performed by using an oxygen sensor (Oxygen Optode 5331, Aanderaa Data Instruments AS, Bergen, Norway) attached to the CTD in every 30 seconds during descent of the cable. The pH of the water sample was determined by using a pH meter. Water samples were kept on ice to limit microbial activity before chemical measurements. Nitrate, nitrite, ammonium, phosphate and dissolved silicate were then analyzed on board by spectrometric methods (Grassholf *et al.*, 1999) within 5 hours after sample collection.

2.2 Analysis of particulate organic carbon (POC), dissolved organic carbon (DOC) and chromophoric dissolved organic matter (CDOM)

Five to ten liters of seawater were filtered through a Whatman GF/F filters (nominal size 0.7 μm, combusted at 450℃ for 4 h prior to use). Filters containing POC were kept frozen until further analysis. The filtrates were added with 5 drops of saturated $HgCl_2$ solution per 100 ml and then kept frozen for measurements of DOC and CDOM. POC samples were thawed at room temperature, soaked in HCl solution (1 M) for 24 h to remove inorganic carbon, dried in low temperature, and packed in tin cups for measurement of total carbon on an elemental analyzer (PerkinElmer 2400 series-II, UC Davis, USA), with deviation smaller than 0.3% for duplicate measurements of each sample. DOC samples were thawed under room temperature and measured via a total organic carbon analyzer linked to an auto-sampler (Shimadzu TOC-L Analyzer, Ocean University of China, China). Samples were acidified with an HCl solution (1 M) and measured three times, with deviation smaller than 4%. Potassium acid phthalate was used as standard substance for DOC quantification.

CDOM was determined for absorbance in a 10-cm quartz cuvette on an ultraviolet and visible spectrophotometer (Shimadzu UV-2550, Ocean University of China, China) at a wavelength internal of 1 nm from 190 nm to 800 nm. Pure water (resistivity = 18.2 MΩ•cm) was used as a reference. The absorbance coefficient representing the relative content of CDOM was calculated using the following equation:

$$a(\lambda) = 2.303/L \times [A(\lambda) - A(\lambda_0)] \quad (1)$$

where $a(\lambda)$ stands for the absorbance coefficient of CDOM at the wavelength of λ (m^{-1}) and $A(\lambda)$ for the absorbance at the wavelength of λ; (λ_0) is the average absorbance at the wavelengths from 695 to 705 nm; and L is the length (m) of the cuvette.

ACCEPTED MANUSCRIPT

Absorbance coefficient of CDOM at the wavelength of 320 nm was applied to represent the relative content of CDOM (Hojerslev and Aas, 2001). As variable volumes of water were filtered for different samples, all the calculations were corrected based on the filtered water volume.

2.3 Isotopic analysis of dissolved inorganic carbon (DIC)

Water was collected (after overflowing ~ 100 ml) in pre-baked 100-ml glass bottles with ground-glass stoppers using pre-cleaned silicone tubing connected directly to the Niskin bottle. After adding 50 μl saturated $HgCl_2$ solution, the bottles were capped tightly with grease-coated ground-glass stoppers and secured with rubber bands to make a gas-tight seal. In the laboratory, DIC was extracted based on the method of Ge *et al.* (2016). Briefly, in a N_2 filled bag, 50 ml water sample was injected into a pre-evacuated 100-ml borosilicate glass bottle with ground-glass-joint stripping probes. After injecting 1.0 ml 85% H_3PO_4, the glass bottle was placed in a 70℃ hot water bath for 30 min and DIC was extracted as CO_2 and collected on the vacuum line, purified cryogenically, and flame-sealed inside 6 mm OD Pyrex tubes for $\Delta^{14}C$ and $\delta^{13}C$ analyses.

Analysis of both $\delta^{13}C$ and $\Delta^{14}C$ of DIC samples was performed at the National Ocean Science Accelerator Mass Spectrometry facilities at Woods Hole Oceanographic Institution. A small split fraction of CO_2 was measured for $\delta^{13}C$ using a VG PRISM isotope ratio mass spectrometry and the remaining of the CO_2 was graphitized for $\Delta^{14}C$ analysis using accelerator mass spectrometry. The precisions of $\Delta^{14}C$-DIC and $\delta^{13}C$-DIC analyses were 5‰ and 0.1‰ or better, respectively (Ge *et al.*, 2016).

DIC concentration was measured using a Shimadzu TOC-L analyzer equipped with an ASI-V auto-sampler, using the total inorganic carbon mode. The concentration of DIC was calibrated using a 5-point calibration curve prepared from reagent grade sodium carbonate and sodium bicarbonate dissolved in DIC-free Milli-Q water as the IC standard. The instrument blank and DIC values were checked against DIC reference material (CRMs, Scripps Institute of Oceanography, University of California San Diego). Total blanks associated with DIC measurements were less than 3.0 μM and the analytic precisions on triplicate injections were < 3%.

2.4 Sampling of microorganisms

Accepted manuscript

ACCEPTED MANUSCRIPT

All water samples were processed on deck. Seawater samples were kept in packed tanks on ice and filtered immediately through 3 μm and subsequently 0.22 μm polycarbonate filters. Material collected on the 0.22 μm filters was considered as small microbial aggregates (SMAs) and material on the 3.0 μm filters large microbial aggregates (LMAs). Filtration was finished within two hours after sample collection. All filters were immediately stored in liquid nitrogen on board of the ship after filtration and then transferred to -80℃ in the laboratory till DNA/RNA extraction. DNA was extracted from the filter samples by using the Mo Bio Laboratories' PowerWater DNA Isolation Kit (MoBio Laboratories, Inc., Carlsbad, California, USA).

2.5 Sequencing and analysis of the 16S rRNA gene amplicons

Samples collected at surface and 500-, 991-, 3699-, 5367-, 7262-, and 8727 mbs were used for high throughput sequencing of the archaeal and bacterial 16S rRNA genes. Specifically, the V4-V5 region of the archaeal 16S rRNA gene and the V3-V4 region of the bacterial 16S rRNA gene were amplified using primers 524F (5′-TGYCAGCCGCCGCGGTAA-3′) / 958R (5′-YCCGGCGTTGAVTCCAATT -3′) and 338F (5′-ACTCCTACGGGAGGCAGCA-3′) / 806R (5′-GGACTACHVGGGTWTCTAAT-3′), respectively. The negative control amplification was conducted using sterile Millio-Q water as template. No positive control was tested. All samples in this study were amplified successfully and there was no band of negative control as detected by gel electrophoresis. Then sequencing was conducted on the Illumina MiSeq platform following the PE300 protocol (MajorBio, China). Sequences generated in this study were deposited at the Sequence Read Archive (SRA) in the National Center for Biotechnology Information (NCBI) under the BioProject accession no. SRP150142, accession No. SRX4189633 - SRX4189660.

Raw sequencing data were quality filtered and analyzed using the pipelines of Quantitative Insights Into Microbial Ecology (Qiime2) (Caporaso *et al.*, 2010). Operational taxonomic units (OTUs) were determined using the DADA2 algorithm (Callahan *et al.*, 2016). OTUs detected only in one sample and with less than five copies were removed. A representative sequence of each OTU was selected for taxonomic identification according to the Silva database (v128) (Quast *et al.*, 2013)

Accepted manuscript

ACCEPTED MANUSCRIPT

and the Greengenes (v13.8) (DeSantis *et al.*, 2006) by Qiime2 with a minimum confidence of 70%. The final annotation was based on the consensus of the results given by these two databases. OTUs classified as chloroplasts were also removed. Phylogeny of the most abundant OTUs were constructed using Raxml (v8.2.11) based on the alignment generated by Sina (v1.2.11) (Pruesse *et al.*, 2012) according to the Silva database (v128). Rarefaction curves of observed OTUs were plotted using Qiime2. Inverse Simpson diversity was evaluated in MOTHUR (Schloss *et al.*, 2009). Statistical analysis of the community dissimilarity based on the Jaccard distance metric and Constrained correspondence analysis (CCA) plotting was conducted using the R package Vegan (v2.4-5) and depth was set as an additional constraint.

2.6 Metagenomic shotgun sequencing and metagenome-assembled 16S rRNA gene analysis

The whole-genome DNA was amplified by using Discover-sc™ Single Cell Kit V2 (Vazyme Biotech, Nanjing, China). 2.5 μl Buffer D1, 1 μl DNA and 1.5 μl deionized water were mixed and then kept at 20 °C for 3 min. 5 μl Buffer N was added, mixed and then kept on ice. The above 10 μl Pre-DN DNA and 40 μl Mix buffer were mixed and kept at 30 °C for 3-6 hours and then 65 °C for 3 minutes. PCR products were then sequenced using the TruSeq® DNA Sample Pre Kit, paired-end library and on an Illumina Genome Analyzer (Hiseq2500, Illumina Inc., San Diego, CA) at Majorbio Bio-Pharm Technology Co., Ltd. (Shanghai, China). 16S rRNA genes were reconstructed using MetaRNA (Huang *et al.*, 2009) and taxonomically annotated as above.

2.7 Microbial activity analysis

Environmental RNA was extracted from the 0.22-μm filters using the RNeasy Mini kit (Qiagen, Hilden, Germany) according to the manufacturer's protocols. DNA fragments were removed from RNA extracts by using the RNase-Free DNase Set (Qiagen, Hilden, Germany). RNA was amplified to test any possible contamination of DNA. Purified RNA was then reverse transcribed to cDNA using the Superscript III First-Strand Synthesis System (Invitrogen, Carlsbad, CA, USA).

The cDNA along with the DNA extraction was amplified with a bacterial universal primer set B8f (5′-AGAGTTTGATCCTGGCTCAG-3′) / B1510 (5′-

Accepted manuscript

ACCEPTED MANUSCRIPT

GGTTACCTTGTTACGACTT-3′). Amplicons were gel-extracted, ligated to the pMD 18-T vector (TaKaRa, Dalian, China) and cloned to *Escherichia coli* JM109. About 100 clones of each sample were randomly selected and sequenced using Applied Biosystems 3730XL. The raw sequences were searched using BLASTN against the NCBI database to remove possible contamination. Chimeric sequences were detected and removed using UCHIME Ref (Edgar *et al.*, 2011). The obtained high-quality sequences (Table S1) were taxonomically assigned with the SILVA database v123 at a minimum support threshold of 80%.

3 Results

3.1 Water temperature and geochemistry

Temperature was about 28.12℃ in surface water. The potential temperature decreased rapidly to 1.86℃ around 2000 mbs (**Fig. 2A**, Table S2). Then it decreased steadily at a much smaller gradient until 8727 mbs, reaching a value of ~1.01℃. DO rapidly decreased in the top 500 mbs (> 200 μM to < 80 μM), which then increased gently to a maximum of ~175 μM at 5000 m, followed by a gentle decrease down to the deep trench (**Fig. 2A**). Water pH decreased from 8.30 at surface to 7.82 at 8727 mbs; salinity increased steadily from 34.31 in surface water to 34.69 at 8727 mbs, except the sharp maximum at 200 mbs (**Fig. 2B**, Table S3).

The surface water was saturated with oxygen but depleted in phosphate, nitrate and DIC concentration (**Fig. 2C, 2D** and **2E**, Table S3). Ammonium was high and had a large variation between surface water (1.81 μM) and water at 3699 mbs (1.33 μM); below this depth, it was low and varied between 0.43 and 0.61 μM (**Fig. 2D**). Nitrate was below 0.5 μM in surface water and varied in the range of 27.73 - 43.10 μM between 991 mbs and 8727 mbs; nitrite was less than 0.1 μM throughout the whole water column (**Fig. 2D**). Phosphate and silicate were lowest in surface water; the former increased to 2.84 μM at 1000 mbs followed by a gentle decrease with depth and the later increased to 161.7 μM at 3699 mbs followed by a gentle decrease with depth (**Fig. 2C**).

DIC concentrations ranged between 1.785-2.236 mM. It was lower (1.785 mM) in the surface and increased rapidly to 2.236 mM at 991 mbs (**Fig. 2E**). Below that, DIC concentrations decreased slightly and remained relatively constant down to 8727 m.

Accepted manuscript

ACCEPTED MANUSCRIPT

The values of $\Delta^{14}C_{DIC}$ and $\delta^{13}C_{DIC}$ ranged in 38‰ to -231‰ and 0.37‰ to -0.7‰, respectively, at the station. $\Delta^{14}C_{DIC}$ decreased rapidly from 38‰ at the surface to -231‰ at 991 mbs and then remained constant down to 8727 mbs. The calculated corresponding ^{14}C ages were modern in the surface down to ~1900 years before present at the deep depths. The depth profile of $\delta^{13}C_{DIC}$ also decreased with depth and the values remained relatively constant at deeper depths.

POC was highest in surface water (5.63 μM) and decreased rapidly to 1.11 μM at 991 mbs. It continued to decrease to 0.58 μM at 3699 mbs and to 0.51 μM at 5367 mbs, after reaching a value of 1.74 μM at 1759 mbs. POC concentration increased again at 8727 mbs to 0.72 μM (**Fi. 2F**). DOC concentration was highest at ocean surface and fluctuated between 37.12 and 45.63 μM at 991 mbs and below (**Fig. 2F**, Table S3). The absorbance coefficient a(320) kept constant at around 0.2 m^{-1} from surface to abyssopelagic depth and was very high (close to 0.5 m^{-1}) at depth 8,727 mbs (**Fig. 2F**).

3.2 Species diversity

We obtained 708,235 16S rRNA gene sequences in total for 14 bacterial and 14 archaeal water samples. Over 99% of the total microbial diversity was successfully captured for all the samples as shown by rarefaction curves of the observed OTUs (Table S4, Fig. S1). Community alpha diversity measured by Inverse Simpson index showed that bacterial diversity was generally greater than archaeal diversity (**Fig. 3**). There was no simple trend in community diversity for SMAs and LMAs. Bacterial diversity in the LMAs remarkably exceeded that in SMAs at depths 2-， 500-, 991- and 7,262 mbs but was comparable between SMAs and LMAs at 8,727 mbs (**Fig. 3**). Total bacterial diversity decreased drastically at 5,367 mbs. At most sampling depths excepting one at 3,699 mbs, archaeal communities in SMAs shared similar diversity with that in LMAs.

3.3 Bacterial community composition at different depths

CCA plots show that surface water bacterial communities and those collected at 991 mbs were remarkably different in composition and each of them was also distant from other samples (**Fig. 4A**). *Prochlorococcus* (B2 and B14), Rhodospirillaceae AEGEAN−169 (B31), *Portiera* (B43), *Marinobacter* (B20 and B22) and *Thalassobius* (B13) were typical surface ocean inhabiting taxa, distinguishable from

Accepted manuscript

ACCEPTED MANUSCRIPT

other samples (**Fig. 4A** and **5**). The surface bacterial communities were significantly correlated to higher temperature and POC but lower DIC, phosphate, silicate concentration and lower salinity ($p < 0.01$).

Below the epipelagic zone (>200 m), Alphaproteobacteria and Gammaproteobacteria constituted the majority of the bacterial community. *Rhodococcus* (B21) and vibrio (B36) were noticeably detected in LMAs at 991 mbs. Additionally, four Oceanospirillales OTUs comprised typical bacterial groups at this depth. DO value was negatively correlated to these taxa (**Fig. 4A**). Deep ocean samples (below 3,000 mbs) were similar in bacterial composition, which was closely related to samples at 500 mbs (Jaccard dissimilarity less than 73% for bacteria and less than 72% for archaea). Exceptions were two Oceanospirillales (B4 and B5), which were abundant at hadal depths of 7,262 and 8,727 mbs (**Fig. 5**). The abundance of a rhodovulum OTU (B1) was remarkable. It comprised up to 54.4% of the bacterial population in deep-ocean samples (see **Section 3.5** and **4.3**).

3.4 Archaeal community composition at different depths

The archaeal fraction of this study was dominated by Marine Group I (MGI), Marine Group II (MGII) and Marine Group III (MGIII) (**Fig. 6**). Compared to the bacterial fraction, archaeal OTU-based sample ordination showed similar patterns between surface and deep ocean samples, except that a high similarity was observed between archaeal communities at 500 and 991 mbs (**Fig. 4B**). Surface microbial communities were in good correlation with higher pH but lower DIC, phosphate and nitrate concentration and lower salinity. They were represented by MGII (A4, A7, A10, A26, A31, A38 and A41) and MGIII (A5, A14 and A52) OTUs. Samples at 500 and 991 mbs were dominated by both MGII/MGIII (e.g. A2, A12, A16 and A36) OTUs and *Nitrosopumilus* (e.g. A30 and A28) OTUs. In deep ocean samples, OTUs from all the three archaeal groups were found.

Vertically, MGI OTUs were only detected below the epipelagic zone (>200 m) (**Fig. 6**). In consistence with Nunoura *et al*. (2015), potential chemoautotrophic *Nitrosopumilus* (phylum Thaumarchaeota, MGI) dominated the sub-surface archaeal population (up to 93.6%, **Fig. 6**). This was in concordance with depleted ammonia in these habitats (**Fig. 2D**). In addition to this overall profile, extensive diversity within these three archaeal groups was discovered. OTUs belonging to different taxonomic subgroups occupied distinct layers of seawater. For example, deep phylogenetic

Accepted manuscript

ACCEPTED MANUSCRIPT

analysis and subgroup assignment showed that the MGI archaeal OTUs belonged to three subgroups (i.e. alpha, gamma and delta) (Fig. S2). Among them, OTUs A1 and A11 of the alpha subgroup, closely related to *Nitrosopumilus maritimus* SCM1 were remarkably and specifically enriched in trench (e.g. A1 with relative abundance 53.74% in SMAs at 8727 mbs) (**Fig. 6**). In contrast, OTUs in the delta groups generally preferred the mesopelagic zone and the members in the gamma groups inhabited either the shallower water or deep ocean.

Habitat specificity was also observed between MGII subgroups (Fig. S3). OTUs of MGII-A were only found in surface water and two MGII-C euryarchaea existed in deep ocean. OTUs of MGII-B were detected in various water depths (**Fig. 6**). Specifically, two MGII-B (A4 and A7) and two MGIII (A5 and A14) OTUs were among the most abundant archaeal populations in SMAs in ocean surface (e.g. A4 with the maximum relative abundance 31.68%) (**Fig. 6**).

3.5 Primer bias validation using metagenomic data

We suspected that the 16S primer bias might have exited in rhodovulum and alteromonas sequence quantification. To address this question, we conducted metagenomic sequencing on SMA and LMA samples at depth 2, 991, 5367, 7,262 and 8,727 mbs and then taxonomically annotated the reads containing 16S rRNA genes. At the genus level, rhodovulum and alteromonas 16S sequences in the metagenomic data comprised 0.75 to 16.6% and 1.1 to 16.6% of all the bacteria in the metagenomic dataset, respectively (Fig. S4). They were 2.1- to 8.8-fold and 0.5- to 6.8-fold less than the amplicon results, respectively. Therefore, amplification bias contributed greatly to over-estimating the rhodovulum population at least at the five depths above. This bias was to a lesser extent in the amplification of alteromonas 16S sequences. We did not remove rhodovulum and alteromonas OTUs from the heatmap (**Fig. 5**) nor from other analyses, since 1) they still comprised a considerable proportion of the bacterial population even after justifying the amplification artifact and 2) it is difficult to tell whether other OTUs were preferentially amplified or not. However, discussion related to rhodovulum and alteromonas was only cautiously made (see **Section 4.3**).

3.6 rRNA abundance versus rRNA gene abundance

To distinguish the autochthonous, metabolically active members of the community, we sequenced the clone libraries of 16S cDNA (reverse complementary rRNA) and

Accepted manuscript

ACCEPTED MANUSCRIPT

16S rRNA genes. Among the most abundant microbial populations, Alphaproteobacteria and Gammaproteobacteria were active at all six depths (Fig. S5). rRNA of cyanobacteria were detected both at the surface and at 8,727 mbs. Only cyanobacterial DNA was found at 1,759 mbs. Cytophagia rRNA were found in considerable amount at all depths but their DNA were only present in low proportions at shallow waters. In addition, rRNA of Flavobacteria, Actinobacteria, Planctomycetacia, Bacilli, and some other bacteria were detected at all depths.

3.7 Partitioning of archaea and bacteria between SMAs and LMAs

The bacterial communities at depth 991 mbs showed greatest dissimilarity (76.02%) between SMA and LMA (Table S5). In deep ocean (depth from 3,699 to 8,727 mbs), dissimilarity between SMA and LMA at each depth was between 59.00% and 69.25%, which was comparable to dissimilarity between samples at different depths (between 58.66% and 72.28%) (**Fig. 4**, Table S5). The greatest dissimilarity (65.63%) between archaeal communities in SMAs and LMAs was observed at 8727 mbs and the lowest (15.00%) was between two surface samples (**Fig. 4**, Table S6). For each of the other deep ocean samples, archaeal community dissimilarity between SMA and LMA fractions was between 48.42% and 52.94%, similar to the dissimilarity between depths (from 48.00% to 68.04%).

4 Discussion

Recent efforts in trench biosphere study have enhanced our understanding of the community structure and potential functions of microorganisms within the deepest ocean (Eloe *et al.*, 2011a; Eloe *et al.*, 2011b; Glud *et al.*, 2013; Yoshida *et al.*, 2013; León-Zayas *et al.*, 2015; Nunoura *et al.*, 2015; Tarn *et al.*, 2016; Nunoura *et al.*, 2016). Yet, limited capability and capacity in sampling hampered this exploration and especially, the temporal dynamics of the microbial communities in global trenches is largely unknown. Our study provides important data that help us in forming the holistic picture of hadal organic matter cycle driven by microorganisms.

4.1 Microbial cells inhabiting different sizes of aggregates

Particle attachment is an important microbial capability for growth and adaptation in the oligotrophic ocean (Tamburini *et al.*, 2013; Orsi *et al.*, 2015). We used the 0.22

Accepted manuscript

ACCEPTED MANUSCRIPT

and 3 μm filter combination for size fractionation of the microbial community. Noticeable but still limited variations in microbial composition between SMAs and LMAs (below 70% for bacteria and below 66% for archaea) was observed in samples collected at the same depth below 1000 mbs (**Fig. 4**, Table S5 and S6). This result was different from those reported in the Puerto Rico Trench (Eloe *et al.*, 2011b) and in the Mariana Trench (Tarn *et al.*, 2016). The lack of strong structural difference of microbial communities might suggest similar nutrient viability in various sizes of particulate matters at the Mariana Trench at our sampling time. Bacterial community diversity was comparable between SMA and LMA at depths 2-, 500-, and 991 mbs while at 7262 mbs microbial diversity of the LMA was much higher in the SMA (**Fig. 3**). This may imply possible increase in particular organic matter (POM) import at this depth at our sampling time (see below). Abundant POM may increase niche diversity and consequently enrich microbial communities associated with these large particles. However, because the POM data is missing at this depth, we are not able to verify this possibility in this study.

4.2 Abundant bacterial heterotrophs in the water columns

In their sampling conducted about seven and half years before ours, Nunoura *et al*. (2015) discovered a surface-to-trench distribution of biochemistry in an oligotrophic area that chemoautotrophs were found in high abundance throughout the deep ocean waters. In contrast, heterotrophs were typically present in the trench, which is relatively nutrient-enriched as a result of lateral transport of organic matter to the trench axis (Ichino *et al.*, 2015). While the report by Nunoura *et al.* (2015) compared community composition at the phylum level, our study presents the most abundant taxonomic lineages in "single-nucleotide resolution" (Callahan *et al.*, 2016) of the ribosomal RNA genes and therefore provides more specific functional prediction between samples.

In general, similar ocean surface populations but noticeably different deep ocean microbial communities were observed in this study compared to previous studies. The surface and shallow water columns (< 1000 mbs) were dominated by photosynthetic planktons (e.g. *Prochlorococcus*, B2 and B14, and a rhodospirillaceae AEGEAN-169, B31) and heterotrophs (**Fig. 5** and **6**). Among them, *Thalassobius* (B13), *Portiera* (B43), *Marinobacter* (B20 and B22) and some MGII and MGIII archaea were only detected in surface water samples, while others could be found in the whole water

ACCEPTED MANUSCRIPT

column we collected, such as *Erythrobacter* (B26), *Shimia* (B18), *Rhodovulum* (B1), rhodobacteraceae (B16 and B19), *Marinobacter* (B15), *Glaciecola* (B23), and *Alteromonas* (B3 and B11). Some of these populations were also detected at the Mariana Trench by Tarn *et al.*, (2016). Although lack of direct evidence, these heterotrophs can be potentially responsible for the initial degradation and transformation of organic carbon fixed by primary producers.

The "unique sequence" approach for OTU generation using DADA2 allowed strain-level ecological analysis of microorganisms (Callahan *et al.*, 2016). At this resolution, we observed microorganisms of the same genus that showed clear habitat partitioning. For example, *Marinobacter* utilize a variety of organic substrates and polycyclic aromatic hydrocarbons as sole carbon sources (Gao *et al.*, 2013). *Marinobacter* B20 and B22 were likely direct consumers of algae/cyanobacteria-released organic carbon in ocean surface, while B30 and B15 were deep-ocean dwelling microbes possibly consuming surface sinking, pre-processed organic matter (**Fig. 5**). Similar pattern of habitat partitioning was also observed in heterotrophic archaeal groups (**Fig. 6**, Fig. S3), in consistence with a previous study in the South China Sea (Liu *et al.*, 2017). Specifically, MGII-A archaea are surface-enriched and MGII-B archaea can be found at various water depths. It was demonstrated that surface water ecotypes of MGII encoded proteorhodopsins, supporting a photoheterotrophic life style, but deep-water populations lacked these proteorhodopsins (Frigaard *et al.*, 2006; Iverson *et al.*, 2012; Zhang *et al.*, 2015; Haro-Moreno *et al.*, 2017; Xie *et al.*, 2017).

Bacteria degrading algal biomass possibly comprised a considerable proportion of the trench microbial community. Some of these heterotrophic groups were also present in ocean surface, implying that this surface-originating organic matter may be an important food source for deep ocean microbes, including those hadal-dwelling ones. Specifically, *Rhodovolum* species are purple nonsulfur bacteria. They are either stenotopic or eurytopic, and can conduct photosynthesis, photoheterotrophy or chemoheterotrophy, in response to changes in environmental conditions (Nupur *et al.*, 2014; Divyasree *et al.*, 2016). They are generally able to degrade aromatic hydrocarbon compounds such as phthalate (Liu and Liu, 2013). *Alteromonas* species are copiotrophic r-strategists. One strain in this genus is a proficient alginolytic bacterium that degrades alginate – a major cell wall polysaccharide from macroalgae (Mitulla *et al.*, 2016). *Glaciecola* are cellulose- and xylan-degraders (Klippel *et al.*, 2011) and *Oceanicola* can also degrade plant cell wall polysaccharide xylan (Kwon *et*

Accepted manuscript

ACCEPTED MANUSCRIPT

al., 2012). *Oleibacter* potentially have high n-alkane-degrading activity (Teramoto *et al.*, 2011). This may imply that the degradation of refractory organic matter is possible in both surface and deep ocean microbial communities (Jiao *et al.*, 2010).

4.3 Unusually high abundance of rhodovulum and alteromonas sequences

With the awareness for primer bias of rhodovulum, we cautiously discuss the unsually high abundance of a rhodovulum OTU (B1) and two alteromonas OTUs (B3 and B11) dominating in the bacterial population of all the samples below surface ocean (**Fig. 5**). Rhodovulum and alteromonas taxa have been frequently isolated from marine environments (Fig. S6). Phylogenetic analysis showed that rhodovulum OTUs (B1, B53 and B106) clustered within a Pacific marine rhodovulum clade and most alteromonas OTUs also clustered with marine-derived sequences, suggesting they were likely true sequences generated from water samples collected at the Mariana Trench (Fig. S6). It is possible, however, that primer bias and 16S operon copy number variation may have led to over-estimation of the rhodovulum and alteromonas OTUs, as indicated by metagenome-derived 16S sequences showing preferential amplification by the primer set (338F/806R) that we used (Fig. S3). Thus quantification of rhodovulum and alteromonas was interpreted with caution in this study.

4.4 Similar microbial communities shared between the hadal zone and the overlain deep ocean water column

With a narrow and elongated topography and great depths from 6000 mbs down to 11000 mbs, trenches are topographically separated from the surrounding abyssal ocean. It is reasonable to speculate that trench microbial communities are distinguishable from those dwelling in the overlain abyssal and bathyal water columns. Nunoura *et al*. (2015 and 2016) suggested a distinct 'trench' sample group from the 'mesopelagic to abyssal' water samples in both trenches. Specifically, the microbial community at 6001 mbs in the Mariana Trench represented a transition point, which showed a connection between the open ocean and the downwards trench habitat (Nunoura *et al.*, 2015). Heterotrophic taxa increased while chemolithoautotrophs decreased in relative abundance in hadal waters.

However, 'trench specificity' was not seen in this study. Instead, a nearly uniform pattern of microbial composition was discovered from the bathypelagic zone down to

ACCEPTED MANUSCRIPT

the hadal waters (**Fig. 5**). In this depth region, no distinguishable change in relative abundance of the dominant OTUs, except some oceanospirillales and nitrosopumilus strains, was observed (**Fig. 5** and **6**). In addition, intra-trench depth stratification of microbial community composition was also absent in our study. Water columns at the upper (7262 mbs) and middle (8727 mbs) depth of the Challenger Deep may have had strong connections with the overlain deep ocean waters (**Fig. 5** and **6**).

Several potential mechanisms may explain this result. First, hadal water is not stagnant but affected by constant hydrological activities, including strong large-scale deep-water currents (Siedler *et al.*, 2004; Kawabe and Fujio, 2010) and internal tides and oscillations (Turnewitsch *et al.*, 2014). Bottom currents may exhibit tidal cycles with semi-lunar and lunar periodicity similarly to those found on abyssal plains (Gould and McKee, 1973). Although typical current speed is low at the Mariana Trench (Taira *et al.*, 2004), strong temporary currents from the abyssal plain may run to the trench and bring planktonic biomass from the overlain water columns. The other possibility is the influence of intensive export of organic matter from the above water columns into the trench. These pulses of organic matter flow along with the microorganisms degrading them might predominately shape the biochemistry of both the bathy-abyssopelagic and hadopelagic water columns, resulting in a homogenized deep ocean microbial community. Lastly, our samples were collected in different seasons of a year (in late December) from Nunoura's (in June). Seasonal environmental difference in illuminance, sea surface temperature, euphotic zone depth, etc. may have direct or indirect effect on the microbial composition of trench waters. These hypotheses, however, have to be validated in future studies.

4.5 Enhanced microbial respiration in the middle of the trench and its possible implications

The typical V-shape cross section of trenches may act as a funnel and could enhance the lateral movement of sediments from the steep slopes towards the axis, resulting in POM accumulation (Itou *et al.*, 2000; Otosaka and Noriki, 2000; Danovaro *et al.*, 2003; Romankevich *et al.*, 2009). This lateral deposition of slope sedimentary organic matter plus the surface sinking organic matter makes the hadal trenches relatively nutrient-enriched compared to the open deep ocean; consequently, trenches can support greater microbial activities (Ichino *et al.*, 2015). In agreement with this hypothesis, a one-fold-higher oxygen consumption rate was measured in sediments of

Accepted manuscript

ACCEPTED MANUSCRIPT

the Mariana Trench (Glud *et al.*, 2013) and the Tonga Trench (Wenzhöfer *et al.*, 2016) compared to their nearby abyssal plains, respectively, indicating enhanced microbial abundance and respiration rate in the trench environment (Glud *et al.*, 2013).

Abundant heterotrophic bacteria detected in trench water in this study (**Fig. 5**) may result in enhanced biodegrading and respiratory activities. Indeed, compared to overlain water columns, the a(320) value of CDOM was significantly higher while the total DOC concentration was lower at 8727 mbs, which is very close to the middle depth (8500 mbs, Fujioka *et al.*, 2002) of the hadal zone of the Challenger Deep (**Fig. 2F**). CDOM in this absorbance range may consist of aromatic and long-chain aliphatic compounds, respectively, which are likely by-products of microbial degradation of DOM as a strong relationship between CDOM and apparent oxygen utilization in the Pacific and Indian Ocean basins was reported before (Nelson and Siegel, 2013). Active microbial respiration and consequently consumption of organic carbon may explain the relatively lower DOC concentration at 8727 mbs (37.12 μM compared to 45.63 μM at 5367 mbs). Although not obvious in the overall vertical DO profile, over 10 μM decrease in DO was observed at 9000 mbs compared to that at 8000 mbs and 5000 mbs (**Fig. 2A**, Table S2). This is in the same scale to the DOC decrease at 8727 mbs. Therefore, we propose that abundant heterotrophs at 8727 mbs might actively degrade organic matter leading to depletion of DOC and accumulation of CDOM.

4.6 Possible temporary fertilization of the oligotrophic Mariana Trench

Primary production in the shallow water zone may significantly affect the distribution and function of deep ocean microbial communities. “Phytodetrital” pulses contribute substantially to the export of both organic carbon and nutritious compounds into the ocean interior (Fabiano *et al.*, 2001; Gibson *et al.*, 2003; Christina and Passow, 2007). The presence of large quantities of labile, phytoplankton-derived compounds in trench sediments confirms that pulses of fresh POM are received occasionally, at least at certain locations (Danovaro *et al.*, 2003). On the other hand, frequent earthquakes in the subduction zone will resuspend sediments on the slopes or abyssal plain and accelerate the focused transportation of organic matter to the trench axis. Consequently, there can be a temporary but significant increase of nutrient in the water columns in the middle of the trench. For example, Kawagucci *et al.* (2012) and Nunoura *et al.* (2016) reported that microbial cell abundance in samples collected at

Accepted manuscript

ACCEPTED MANUSCRIPT

depth between 5500 and 5750 mbs 35 days after the Tohoku Earthquake was outstandingly higher than that of other abyssal to hadal samples, including samples collected at the same depth but 96 days after the earthquake. This temporary boost of biomass might be the result of lateral input of sedimentary OM from adjacent abyssal plain, which were suspended by the vibration during the earthquake. Meanwhile, this nutrient flux might be efficiently consumed by this microbial flourish before sinking down to the trench depth. Surface waters in oligotrophic regions are dominated by picophytoplankton, which may form aggregates exhibiting sinking speeds comparable to those of large algae (e.g. in the form of "marine snow") and may contribute equally to surface carbon export (Richardson and Jackson, 2007). Small autofluorescent coccoid cyanobacteria were found notably abundant in deep-sea phytodetritus (Lochte and Turley, 1988; Beaulieu and Smith, 1998).

Cyanobacterial aggregates may enhance phytodetrital flux as picophytoplankton RNA sequences were detected in remarkable abundance in the hadal zone (**Fig. 5** and Fig. S5), which were most likely originated from surface-fast-sinking cells (Eloe *et al.*, 2011b). It is possible that temporary pules of phytodetritus may export organic matter in the form of POM to the deep ocean and reshape *in situ* nutrient quantity and quality and consequently, microbial communities. Growth of heterotrophic bacteria may be promoted (**Fig. 5**). This influx of organic matter may erase the community difference between the interior trench and the abyssal plain, resulting in a nearly uniform deep ocean microbial profile.

Conclusions

Our study presents the latest vertical profiling of the planktonic microbial community at the Marina Trench, which is the deepest ocean on Earth. Similar heterotrophic microbial communities were observed in deep ocean including the hadal zone. Many of these heterotrophs were also detected in ocean surface. Some deep sea-enriched microorganisms are characterized by the ability to degrade large organic polymers. Elevated levels of chromophoric dissolved organic matter were detected at the middle zone of the hadal trench implying higher microbial activity. These results suggest a potentially unusual state of the Mariana Trench compared to the previous study (Nunoura *et al.*, 2015). However, the logistical difficulties in sampling at the Mariana Trench and ship time limitation only allowed us to conduct detailed vertical sampling

Accepted manuscript

ACCEPTED MANUSCRIPT

at one station. This limits the robustness of the findings of this study. Extraordinary efforts in future cruises are needed to fully validate these observations.

Acknowledgements

This research cannot be accomplished without the professional support from the captain and crew of the R/V Dongfanghong 2; special thanks are due to Mr. Sun and his team for each successful operation of the demanding CTD deployment. We appreciate the comments from Takuro Nunoura, which helped improve the quality of the paper. We also thank Jose Manuel Haro Moreno for his help on analyzing metagenomics data. This research was supported by the Fourth Polar Observation Program (i.e. Deep Sea Exploration Program, Qingdao National Laboratory for Marine Science & Technology)-Cruise 2016, National Key Basic Research Program of China (Program 973) [grant number 2014CB745003], the comprehensive survey in winter at the Southern West Pacific [grant number GASI-02-PAC-ST-MSwin], Global Change and Air-Sea Interaction Project [grant number GASI-IPOVAI-01-03], the Fourth Polar Observation Program (i.e. Deep Sea Exploration Program, Qingdao National Laboratory for Marine Science & Technology)-Cruise 2017, the Fundamental Research Funds for the Central Universities [grant number 201762009, XCW], the National Natural Science Foundation of China [grants numbers 41530105, 91428308, 41373072], the Southern University of Science and Technology [grant number Y01316209], the Shenzhen Key Laboratory of Marine Archaea Geo-Omics, Southern University of Science and Technology, and the Laboratory for Marine Geology, Qingdao Pilot National Laboratory for Marine Science and Technology [CLZ].

Accepted manuscript

Author contributions

J.T. and C.L.Z conceived the study. J.T. and H.L. collected the microbial samples and proceeded them for sequencing. L.F., H.L., J.L., D.B., X.Z. and C.L.Z performed bioinformatic analyses. Y.L., Q.Q., Z.G., H.C., Z.S., L.Z., X.W., H.X., M.W. and Y.Z. conducted the chemical and physical measurements. L.F., H.L. and C.L.Z wrote and all authors edited and approved the manuscript.

ACCEPTED MANUSCRIPT

Competing interests

The authors declare no competing interests.

References

1. Beaulieu, S.E. and Smith, K.L. (1998). Phytodetritus entering the benthic boundary layer and aggregated on the sea floor in the abyssal NE Pacific: macro-and microscopic composition. *Deep-Sea Res Pt II.* 45, 781-815.
2. Callahan, B.J., McMurdie, P.J., Rosen, M.J., Han, A.W., Johnson, A.J., Holmes, S.P. (2016). DADA2: High-resolution sample inference from Illumina amplicon data. *Nat Methods.* 13, 581-583. doi: 10.1038/nmeth.386
3. Caporaso, J.G., Kuczynski, J., Stombaugh, J., Bittinger, K., Bushman, F.D., Costello, E.K., et al. (2010). QIIME allows analysis of high-throughput community sequencing data. *Nat Methods.* 7, 335-336. doi: 10.1038/nmeth.f.303
4. Christina, L. and Passow, U. (2007). Factors influencing the sinking of POC and the efficiency of the biological carbon pump. *Deep-Sea Res Pt II.*. 54, 639-658.
5. Danovaro, R., Della Croce, N., DellAnno, A., Pusceddu, A. (2003). A depocenter of organic matter at 7800m depth in the SE Pacific Ocean. *Deep-Sea Res Pt I.* 50, 1411-1420.
6. DeSantis, T.Z., Hugenholtz, P., Larsen, N., Rojas, M., Brodie, E.L., Keller, K., et al. (2006). Greengenes, a chimera-checked 16S rRNA gene database and workbench compatible with ARB. *Appl Environ Microbiol.* 72**,** 5069-5072.
7. Divyasree, B., Lakshmi, K.V., Bharti, D., Sasikala, C.h., Ramana, C.h.V. (2016). *Rhodovulum aestuarii* sp. nov., isolated from a brackish water body. *Int J Syst Evol Microbiol.* 66, 165-171. doi: 10.1099/ijsem.0.000691
8. Edgar, R.C., Haas, B.J., Clemente, J.C., Quince, C., Knight, R. (2011). UCHIME improves sensitivity and speed of chimera detection. *Bioinformatics.* 27, 2194-2200. doi: 10.1093/bioinformatics/btr381
9. Eloe, E.A., Fadrosh, D.W., Novotny, M., Zeigler Allen, L., Kim, M., Lombardo, M.J., et al. (2011a). Going deeper: metagenome of a hadopelagic microbial community. *PLoS One.* 6, e20388. doi: 10.1371/journal.pone.0020388

Accepted manuscript

ACCEPTED MANUSCRIPT

10. Eloe, E.A., Shulse, C.N., Fadrosh, D.W., Williamson, S.J., Allen, E.E., Bartlett, D.H. (2011b). Compositional differences in particle-associated and free-living microbial assemblages from an extreme deep-ocean environment. *Environ Microbiol Rep.* 3, 449-458. doi: 10.1111/j.1758-2229.2010.00223.x
11. Fabiano, M., Pusceddu, A., Dell'Anno, A., Armeni, M., Vanucci, S., Lampitt, R.S., et al. (2001). Fluxes of phytopigments and labile organic matter to the deep ocean in the NE Atlantic Ocean. *Prog Oceanog.* 50, 89-104.
12. Frigaard, N.U., Martinez, A., Mincer, T.J., DeLong, E.F. (2006). Proteorhodopsin lateral gene transfer between marine planktonic Bacteria and Archaea. *Nature.* 439, 847-850. doi: 10.1038/nature04435
13. Fujii, T., Kilgallen, N.M., Rowden, A.A., Jamieson, A.J. (2013). Deep-sea amphipod community structure across abyssal to hadal depths in the Peru-Chile and Kermadec trenches. *Mar Ecol Prog Ser.* 492, 125-138.
14. Fujioka K, Okino K, Kanamatsu T, Ohara Y. (2002). Morphology and origin of the Challenger Deep in the Southern Mariana Trench. *Geoph Res Lett*. 29, 1737-1740.
15. Gallo, N.D., Cameron, J., Hardy, K., Fryer, P., Bartlett, D.H., Levin, L.A. (2015). Submersible-and lander-observed community patterns in the Mariana and New Britain trenches: influence of productivity and depth on epibenthic and scavenging communities. *Deep-Sea Res Pt I.* 99, 119-133.
16. Gao, W., Cui, Z., Li, Q., Xu, G., Jia, X., Zheng, L. (2013). *Marinobacter nanhaiticus* sp. nov., polycyclic aromatic hydrocarbon-degrading bacterium isolated from the sediment of the South China Sea. *Antonie Van Leeuwenhoek.* 103, 485-491. doi: 10.1007/s10482-012-9830-z
17. Ge, T., Wang, X., Zhang, J., Luo, C., Xue, Y. (2016). Dissolved inorganic radiocarbon in the northwest Pacific continental margin. *Radiocarbon.* 58, 517-529.
18. Gibson, R.N., Barnes, M., Atkinson, R.J.A. (2003). Accumulation and fate of phytodetritus on the sea floor. *Oceanog and Mar Bio.* 40, 171.
19. Glud, R.N., Wenzhöfer, F., Middelboe, M., Oguri, K., Turnewitsch, R., Canfield, D.E., et al. (2013). High rates of microbial carbon turnover in sediments in the deepest oceanic trench on Earth. *Nat Geosci.* 6, 284-288.
20. Gould, W.J. and McKee, W.D. (1973). Vertical structure of semi-diurnal tidal currents in the Bay of Biscay. *Nature.* 244, 88-91.

Accepted manuscript

ACCEPTED MANUSCRIPT

21. Grassholf K., Kremling K., Ehrhardt M. (1999). Methods of seawater analysis, 3rd ed. Verlag Chemie GmbH D-6940: Weinheim.
22. Haro-Moreno, J. M., Rodriguez-Valera, F., Lopez-Garcia, P., Moreira, D., & Martin-Cuadrado, A. B. (2017). New insights into marine group iii euryarchaeota, from dark to light. *ISME J*, 11, 1102-1117.
23. Hojerslev, N.K. and Aas, E. (2001). Spectral light absorption by yellow substance in the Kattegat-Skagerrak area. *Oceanologia.* 43.
24. Huang, Y., Gilna, P., Li, W. (2009). Identification of ribosomal RNA genes in metagenomic fragments. *Bioinformatics*. 25, 1338-1340.
25. Ichino, M.C., Clark, M.R., Drazen, J.C., Jamieson, A., Jones, D.O., Martin, A.P., et al. (2015). The distribution of benthic biomass in hadal trenches: a modelling approach to investigate the effect of vertical and lateral organic matter transport to the seafloor. *Deep-Sea Res Pt I.* 100, 21-33.
26. Itou, M., Matsumura, I., Noriki, S. (2000). A large flux of particulate matter in the deep Japan Trench observed just after the 1994 Sanriku-Oki earthquake. *Deep-Sea Res Pt I.* 47, 1987-1998.
27. Iverson, V., Morris, R.M., Frazar, C.D., Berthiaume, C.T., Morales, R.L., Armbrust, E.V. (2012). Untangling genomes from metagenomes: revealing an uncultured class of marine euryarchaeota. *Science.* 335, 587-590. doi: 10.1126/science.1212665
28. Jiao, N., Herndl, G.J., Hansell, D.A., Benner, R., Kattner, G., Wilhelm, S.W., et al. (2010). Microbial production of recalcitrant dissolved organic matter: long-term carbon storage in the global ocean. *Nat Rev Microbiol.* 8, 593-599. doi: 10.1038/nrmicro2386
29. Kawabe, M. and Fujio, S. (2010). Pacific Ocean circulation based on observation. *J Oceanog.* 66, 389.
30. Kawagucci, S., Yoshida-Takashima, Y., Noguchi, T., Honda, M. C., Uchida, H., Ishibashi, H., et al. (2012). Disturbance of deep-sea environments induced by the M9.0 Tohoku earthquake. *Sci Rep.* 2, 270.doi:10.1038/srep 00270
31. Klippel, B., Lochner, A., Bruce, D.C., Davenport, K.W., Detter, C., Goodwin, L.A., et al. (2011). Complete genome sequence of the marine cellulose- and xylan-degrading bacterium *Glaciecola* sp. strain 4H-3-7+YE-5. *J Bacteriol*. 193, 4547-4548.

Accepted manuscript

ACCEPTED MANUSCRIPT

32. Kwon, Y.K., Kim, J.J., Kim, J.H., Jeon, S.M., Ye, B.R., Jang, J., et al. (2012). Draft genome sequence of the xylan-degrading marine bacterium strain S124, representing a novel species of the genus Oceanicola. *J Bacteriol.* 194, 6325. doi: 10.1128/JB.01614-12

33. Lacey, N.C., Rowden, A.A., Clark, M.R., Kilgallen, N.M., Linley, T., Mayor, D.J., et al. (2016). Community structure and diversity of scavenging amphipods from bathyal to hadal depths in three South Pacific Trenches. *Deep-Sea Res Pt I.* 111, 121-137.

34. Lauro, F.M. and Bartlett, D.H. (2008). Prokaryotic lifestyles in deep sea habitats. *Extremophiles.* 12, 15-25. doi: 10.1007/s00792-006-0059-5

35. León-Zayas, R., Novotny, M., Podell, S., Shepard, C.M., Berkenpas, E., Nikolenko, S., et al. (2015). Single cells within the Puerto Rico trench suggest hadal adaptation of microbial lineages. *Appl Environ Microbiol.* 81, 8265-8276. doi: 10.1128/AEM.01659-15.

36. Liu, H., Zhang, C.L., Yang, C., Chen, S., Cao, Z., Zhang, Z., et al. (2017). Marine group II dominates planktonic archaea in water column of the Northeastern South China Sea. *Front Microbiol.* 8, 1098. doi: 10.3389/fmicb.2017.01098.

37. Liu, R., Wang, L., Wei, Y., and Fang, J. (2017). The hadal biosphere: Recent insights and new directions. *Deep-Sea Res Pt II.* (in press) doi.org/10.1016/j.dsr2.2017.04.015.

38. Liu, Z. and Liu, J. (2013). Evaluating bacterial community structures in oil collected from the sea surface and sediment in the northern Gulf of Mexico after the Deepwater Horizon oil spill. *Microbiologyopen.* 2, 492-504. doi: 10.1002/mbo3.89

39. Lochte, K. and Turley, C.M. (1988). Bacteria and cyanobacteria associated with phytodetritus in the deep sea. *Nature.* 333, 67-69.

40. Mitulla, M., Dinasquet, J., Guillemette, R., Simon, M., Azam, F., Wietz, M. (2016). Response of bacterial communities from California coastal waters to alginate particles and an alginolytic *Alteromonas macleodii* strain. *Environ Microbiol.* 18, 4369-4377. doi: 10.1111/1462-2920.13314

41. Moeseneder, M.M., Winter, C., Herndl, G.J. (2001). Horizontal and vertical complexity of attached and free-living bacteria of the eastern Mediterranean

Accepted manuscript

ACCEPTED MANUSCRIPT

Sea, determined by 16S rDNA and 16S rRNA fingerprints. *Limnol Oceanog.* 46, 95-107.

42. Nelson, N.B. and Siegel, D.A. (2013). The global distribution and dynamics of chromophoric dissolved organic matter. *Ann Rev Mar Sci.* 5, 447-476. doi: 10.1146/annurev-marine-120710-100751
43. Nunoura, T., Hirai, M., Yoshida-Takashima, Y., Nishizawa, M., Kawagucci, S., Yokokawa, T., et al. (2016). Distribution and niche separation of planktonic microbial communities in the water columns from the surface to the hadal waters of the Japan Trench under the eutrophic ocean. *Front Microbiol.* 7, 1261. doi: 10.3389/fmicb.2016.01261
44. Nunoura, T., Takaki, Y., Hirai, M., Shimamura, S., Makabe, A., Koide, O., et al. (2015). Hadal biosphere: insight into the microbial ecosystem in the deepest ocean on Earth. *Proc Natl Acad Sci U S A.* 112, E1230-E1236. doi: 10.1073/pnas.1421816112
45. Nupur, P., Srinivas, T.N., Takaichi, S., Anil Kumar, P. (2014). *Rhodovulum mangrovi* sp. nov., a phototrophic alphaproteobacterium isolated from a mangrove forest sediment sample. *Int J Syst Evol Microbiol.* 64, 3168-3173. doi: 10.1099/ijs.0.059857-0
46. Oguri, K., Kawamura, K., Sakaguchi, A., Toyofuku, T., Kasaya, T., Murayama, M., et al. (2013). Hadal disturbance in the Japan Trench induced by the 2011 Tohoku-Oki earthquake. *Sci Rep.* 3, 1915. doi: 10.1038/srep01915
47. Orsi, W.D., Smith, J.M., Wilcox, H.M., Swalwell, J.E., Carini, P., Worden, A.Z., et al. (2015). Ecophysiology of uncultivated marine euryarchaea is linked to particulate organic matter. *ISME J.* 9, 1747-1763. doi: 10.1038/ismej.2014.260
48. Otosaka, S. and Noriki, S. (2000). REEs and Mn/Al ratio of settling particles: horizontal transport of particulate material in the northern Japan Trench. *Mar Chem.* 72, 329-342.
49. Partensky, F., Hess, W.R., Vaulot, D. (1999). Prochlorococcus, a marine photosynthetic prokaryote of global significance. *Microbiol Mol Biol Rev.* 63, 106-127.
50. Pruesse, E., Peplies, J. and Glöckner, F.O. (2012) SINA: accurate high-throughput multiple sequence alignment of ribosomal RNA genes. *Bioinformatics*, 28, 1823-1829.

Accepted manuscript

ACCEPTED MANUSCRIPT

51. Quast, C., Pruesse, E., Yilmaz, P., Gerken, J., Schweer, T., Yarza, P., et al. (2013). The SILVA ribosomal RNA gene database project: improved data processing and web-based tools. *Nucleic Acids Res.* 41, D590-D596. doi: 10.1093/nar/gks1219

52. Reinthaler, T., Van Aken, H., Veth, C., Arístegui, J., Robinson, C., Williams, P.J.L.B., et al. (2006). Prokaryotic respiration and production in the meso-and bathypelagic realm of the eastern and western North Atlantic basin. *Limnol Oceanog.* 51, 1262-1273.

53. Richardson, T.L. and Jackson, G.A. (2007). Small phytoplankton and carbon export from the surface ocean. *Science.* 315, 838-840. doi: 10.1126/science.1133471

54. Romankevich, E.A., Vetrov, A.A., Peresypkin, V.I. (2009). Organic matter of the World Ocean. *Russ Geol Geoph.* 50, 299-307.

55. Ruhl, H.A., Ellena, J.A., Smith, K.L. (2008). Connections between climate, food limitation, and carbon cycling in abyssal sediment communities. *Proc Natl Acad Sci U S A.* 105, 17006-17011. doi: 10.1073/pnas.0803898105

56. Ruhl, H.A. and Smith, K.L. (2004). Shifts in deep-sea community structure linked to climate and food supply. *Science.* 305, 513-515. doi: 10.1126/science.1099759

57. Schloss, P.D., Westcott, S.L., Ryabin, T., Hall, J.R., Hartmann, M., Hollister, E.B., et al. (2009). Introducing mothur: open-source, platform-independent, community-supported software for describing and comparing microbial communities. *Appl Environ Microbiol.* 75, 7537-7541. doi: 10.1128/AEM.01541-09

58. Siedler, G., Holfort, J., Zenk, W., Müller, T.J., Csernok, T. (2004). Deep-water flow in the Mariana and Caroline Basins. *J Phys oceanog.* 34, 566-581.

59. Taira, K., Kitagawa, S., Yamashiro, T., Yanagimoto, D. (2004). Deep and bottom currents in the Challenger Deep, Mariana Trench, measured with super-deep current meters. *J Oceanog.* 60, 919-926.

60. Tamburini, C., Boutrif, M., Garel, M., Colwell, R. R., & Deming, J. W. (2013). Prokaryotic responses to hydrostatic pressure in the ocean--a review. *Environ Microbiol.* 15, 1262-74.

61. Tarn, J., Peoples, L.M., Hardy, K., Cameron, J., Bartlett, D.H. (2016). Identification of free-living and particle-associated microbial communities

Accepted manuscript

ACCEPTED MANUSCRIPT

present in hadal regions of the Mariana Trench. *Front Microbiol.* 7, 665. doi: 10.3389/fmicb.2016.00665

62. Teramoto, M., Ohuchi, M., Hatmanti, A., Darmayati, Y., Widyastuti, Y., Harayama, S., et al. (2011). *Oleibacter marinus* gen. nov., sp. nov., a bacterium that degrades petroleum aliphatic hydrocarbons in a tropical marine environment. *Int J Syst Evol. Microbiol.* 61, 375-380. doi: 10.1099/ijs.0.018671-0
63. Turnewitsch, R., Falahat, S., Stehlikova, J., Oguri, K., Glud, R.N., Middelboe, M., et al. (2014). Recent sediment dynamics in hadal trenches: Evidence for the influence of higher-frequency (tidal, near-inertial) fluid dynamics. *Deep-Sea Res Pt I.* 90, 125-138.
64. Wenzhöfer, F., Oguri, K., Middelboe, M., Turnewitsch, R., Toyofuku, T., Kitazato, H., et al. (2016). Benthic carbon mineralization in hadal trenches: assessment by in situ O 2 microprofile measurements. *Deep-Sea Res Pt I.* 116, 276-286.
65. Xie, W., Luo, H., Murugapiran, S. K., Dodsworth, J. A., Chen, S., & Sun, Y., et al. (2017). Localized high abundance of marine group ii archaea in the subtropical pearl river estuary: implications for their niche adaptation. *Environ Microbiol*. 20:734-754. doi:10.1111/1462-2920.14004
66. Yoshida, M., Takaki, Y., Eitoku, M., Nunoura, T., Takai, K. (2013). Metagenomic analysis of viral communities in (hado)pelagic sediments. *PLoS One.* 8, e57271. doi: 10.1371/journal.pone.0057271
67. Zhang, C.L., Xie, W., Martin-Cuadrado, A.B., and Rodriguez-Valera, F. (2015). Marine Group II Archaea, potentially important players in the global ocean carbon cycle. *Front Microbiol.* 6, 1108. doi: 10.3389/fmicb.2015.01108

Accepted manuscript

Fig. 1. Geographic position of the sampling site. Sampling site of this study and two previous studies: N2015 (Nunoura *et al.*, 2015) and T2016 (Tarn *et al.*, 2016). B is a zoomed in picture of A.

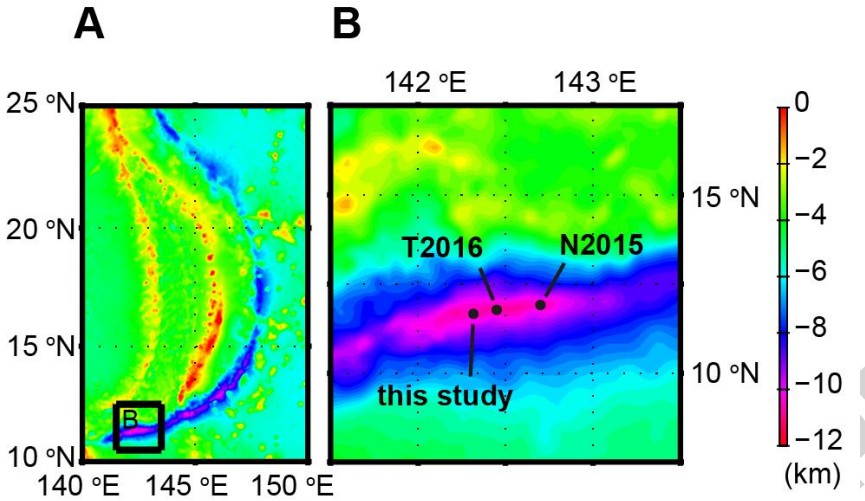

Accepted manuscript

ACCEPTED MANUSCRIPT

Fig. 2. Physical and Chemical measurements of the sampling site. Data from this study are presented as circles and data from the study by Nunoura *et al.* (2015) are presented as dots. A, temperature and DO; B, salinity and pH; C, silicate and phosphate; D, nitrogen species; E, DIC; and F, organic matter.

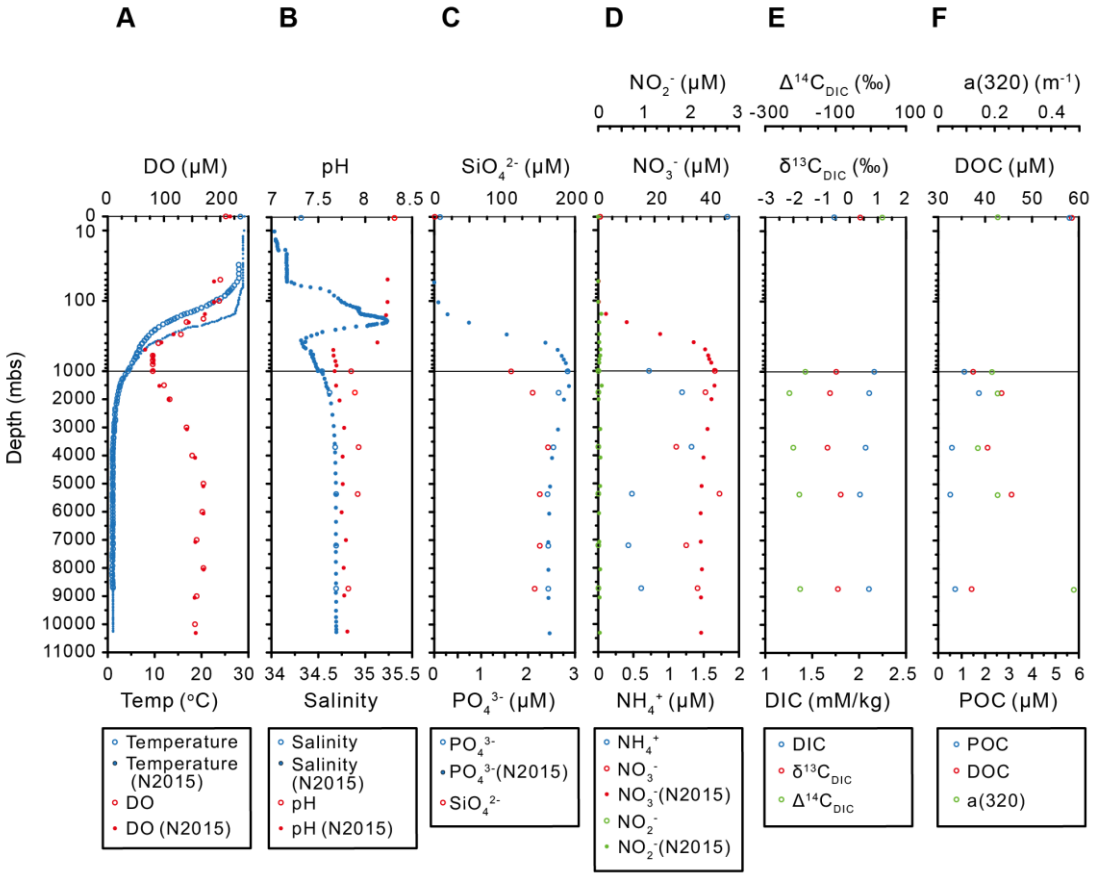

Accepted

ACCEPTED MANUSCRIPT

Fig. 3. Bacterial and archaeal alpha diversity. Data from this study are presented as circles. OTU alpha diversity is calculated as the Inverse-Simpson Index. The arrow indicate the actual position of the purple circle at depth 5367 mbs.

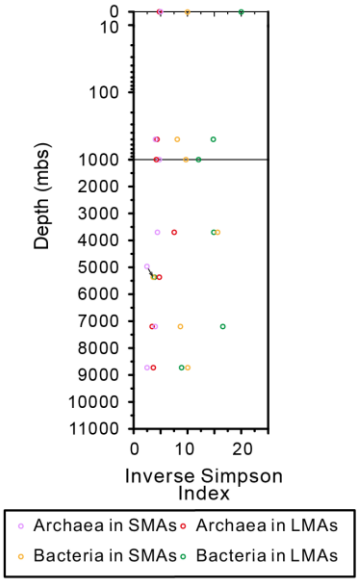

Accepted manuscript

ACCEPTED MANUSCRIPT

Fig. 4. CCA plotting showing community composition dissimilarity between samples. A, based on the bacterial proportion; B, based on the archaeal proportion. MGI, marine group I. MGII, marine group II. MGIII, marine group III. Blue dots present samples in the fraction of LMAs while blue circles present samples in the fraction of SMAs. Labels of blue dots and circles indicate depth as meters below ocean surface. Plotting is based on Jaccard distance matrix with depth as an additional constraint. As our prior assumption is that depth was the ultimate cause of chemical and microbial stratification, depth's constraint was intentionally shown on the x-axis by force and the first constraint without depth's effect was shown on the y-axis. Effective environmental factors (p value < 0.01) are fitted to the ordination. Black asterisks show OTUs. OTUs showed in **Fig. 5** and **Fig. 6** are taxonomically labelled here.

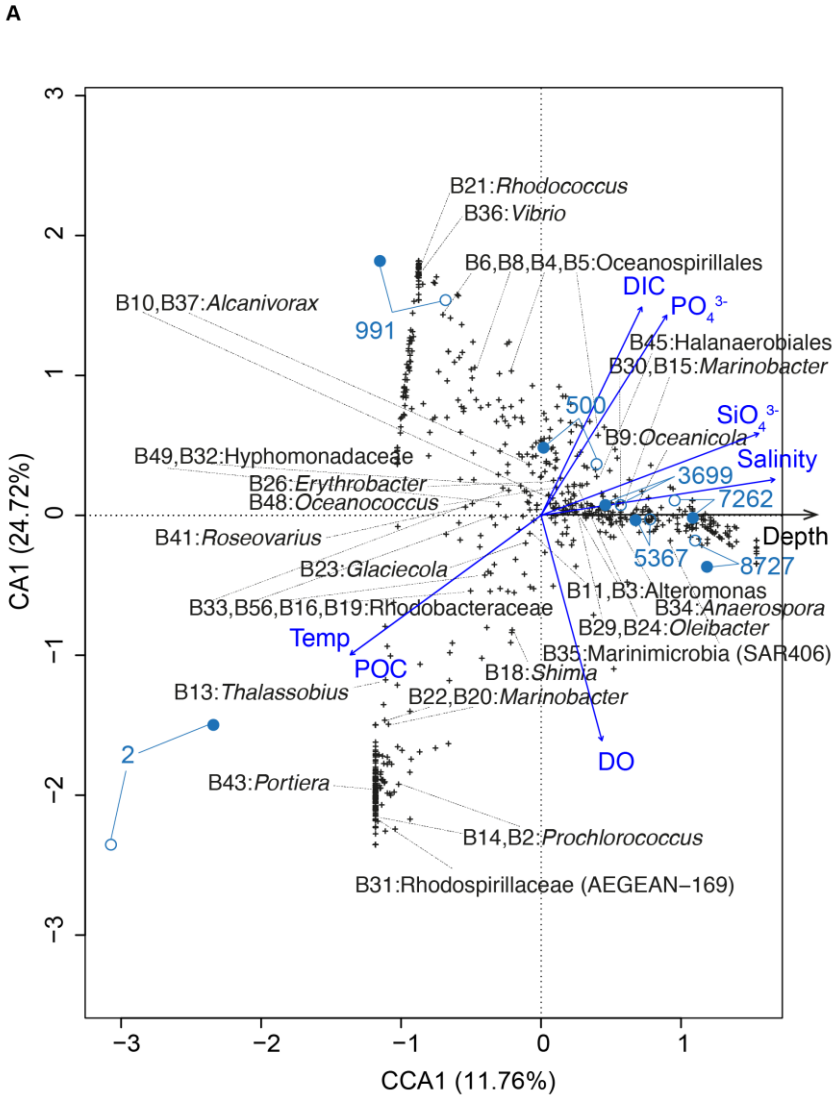

B

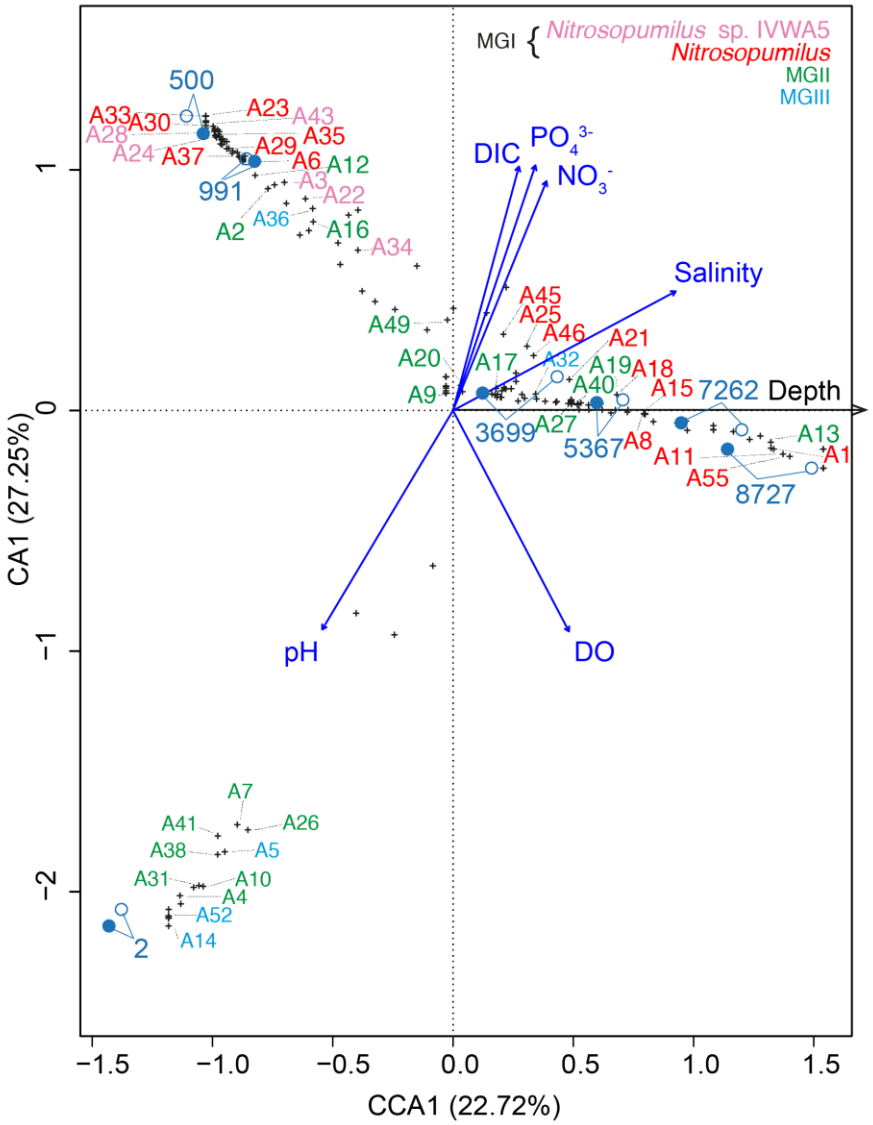
MGI
Nitrosopumilus sp. IVWA5
Nitrosopumilus
MGII
MGIII
DIC
PO4 3-
NO3 -
Salinity
pH
DO
Depth
CA1 (27.25%)
CCA1 (22.72%)
500
991
2
3699
5367
7262
8727
A1
A2
A3
A4
A5
A6
A7
A8
A9
A10
A11
A12
A13
A14
A15
A16
A17
A18
A19
A20
A21
A22
A23
A24
A25
A26
A27
A28
A29
A30
A31
A32
A33
A34
A35
A36
A37
A38
A40
A41
A43
A45
A46
A49
A52
A55

Accepted

ACCEPTED MANUSCRIPT

Fig. 5. Relative abundance of bacterial OTUs. γ, Gammaproteobacteria. α, Alphaproteobacteria. OTUs with maximum (among the 14 samples) abundance greater than 1.5% are shown. The phylogenetic tree was rooted to the midpoint. Node confidence values are based on 1000 bootstraps. Only values > 50 are shown.

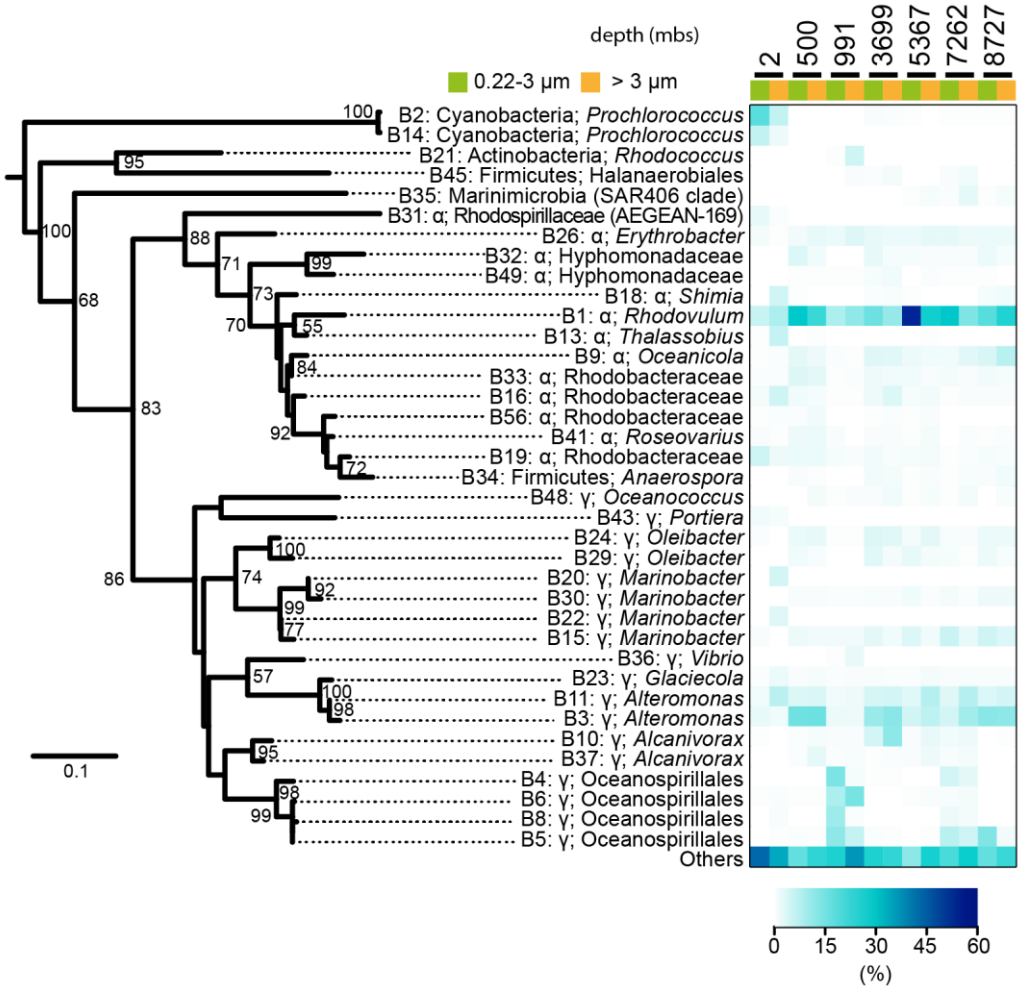

Fig. 6. Relative abundance of archaeal OTUs. MGI, marine group I. MGII, marine group II. MGIII, marine group III. OTUs with maximum (among the 14 samples) abundance greater than 2% are shown. The phylogenetic tree was rooted to the midpoint. Node confidence values are based on 1000 bootstraps. Only values > 50 are shown.

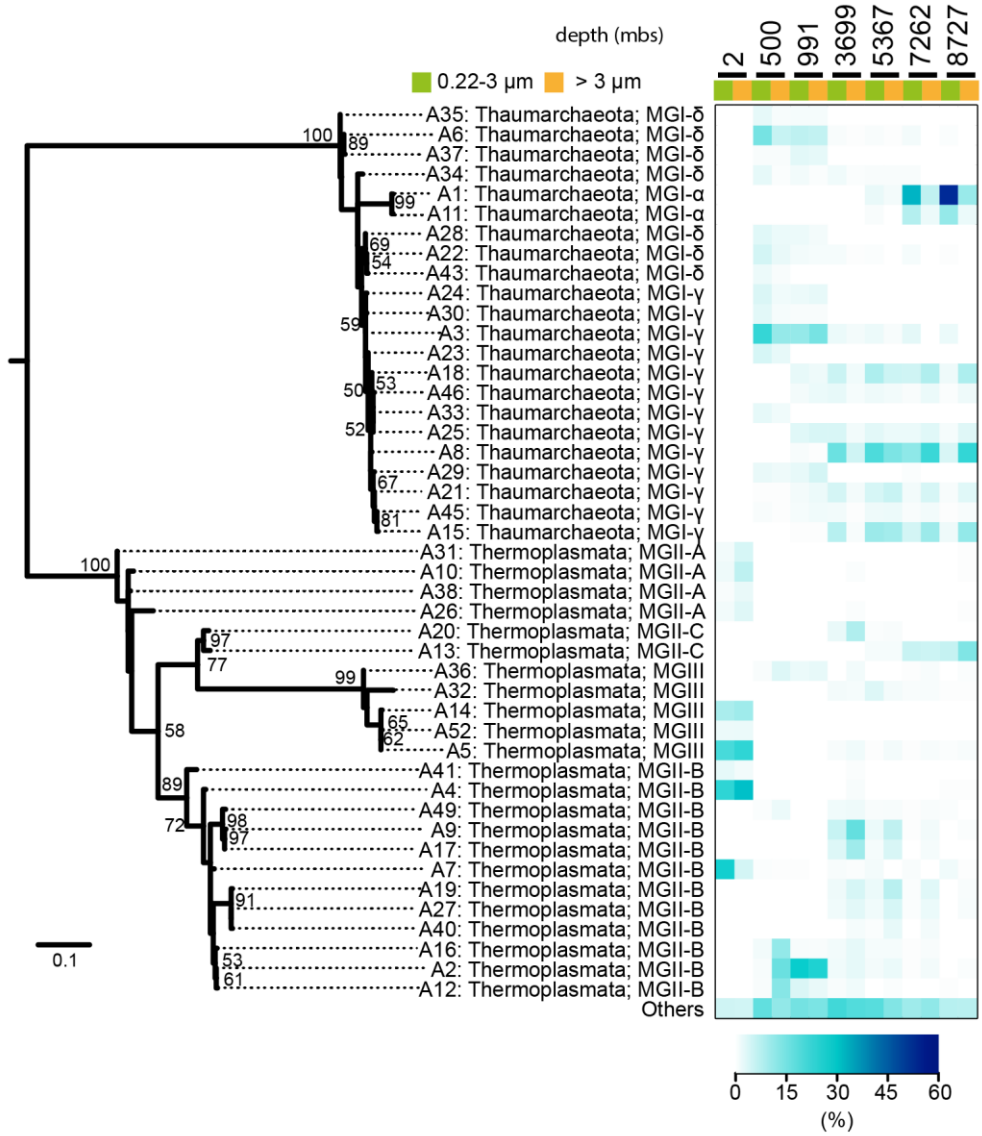

ACCEPTED MANUSCRIPT

Highlights

- Abundant bacterial heterotrophs were detected below 1000 m of the Mariana Trench
- Nearly uniformed microbial composition in the hadal zone and the overlain deep ocean
- Community difference between differently-sized aggregates was insignificant
- DOC variation suggests active microbial respiration in the hadal zone
- Some deep-sea-enriched bacteria are potential degraders of large organic polymers

Accepted manuscript